

# Flexible Self-Powered GaN Ultraviolet Photoswitch with Piezo-Phototronic Effect Enhanced On/Off Ratio

Mingzeng Peng,<sup>†</sup> Yudong Liu,<sup>†</sup> Aifang Yu,<sup>†</sup> Yang Zhang,<sup>†</sup> Caihong Liu,<sup>†</sup> Jingyu Liu,<sup>†</sup> Wei Wu,<sup>†</sup> Ke Zhang,<sup>†</sup> Xieqing Shi,<sup>†</sup> Jinzong Kou,<sup>†</sup> Junyi Zhai,<sup>\*,†</sup> and Zhong Lin Wang<sup>\*,†,‡</sup>

<sup>†</sup>Beijing Institute of Nanoenergy and Nanosystems, Chinese Academy of Sciences, Beijing 100083, China

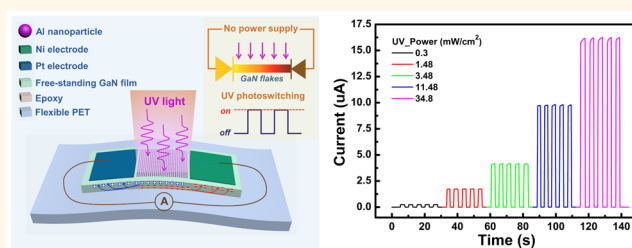
<sup>‡</sup>School of Materials Science and Engineering, Georgia Institute of Technology, Atlanta, Georgia 30332-0245, United States

## Supporting Information

**ABSTRACT:** Flexible self-powered sensing is urgently needed for wearable, portable, sustainable, maintenance-free and long-term applications. Here, we developed a flexible and self-powered GaN membrane-based ultraviolet (UV) photoswitch with high on/off ratio and excellent sensitivity. Even without any power supply, the driving force of UV photogenerated carriers can be well boosted by the combination of both built-in electric field and piezoelectric polarization field. The asymmetric metal–semiconductor–metal structure has been elaborately utilized to enhance the

carrier separation and transport for highly sensitive UV photoresponse. Its UV on/off ratio and detection sensitivity reach to  $4.67 \times 10^5$  and  $1.78 \times 10^{12} \text{ cm} \cdot \text{Hz}^{0.5} \text{ W}^{-1}$ , respectively. Due to its excellent mechanical flexibility, the piezoelectric polarization field in GaN membrane can be easily tuned/controlled based on piezo-phototronic effect. Under 1% strain, a stronger and broader depletion region can be obtained to further enhance UV on/off ratio up to 154%. As a result, our research can not only provide a deep understanding of local electric field effects on self-powered optoelectronic detection, but also promote the development of self-powered flexible optoelectronic devices and integrated systems.

**KEYWORDS:** self-powered, flexible optoelectronic sensing, UV photoswitch, piezo-phototronic, on/off ratio



Sensor networks are a key technological and economic driver for global industries in the near future with wide-range of applications in internet of things, environmental monitoring, health care, infrastructure monitoring, national security, and so on.<sup>1,2</sup> One of the major problems in sensor networks is the electric power needed to drive individual sensors for sustainable and maintenance-free operation. Meanwhile, realization of optoelectronic sensing with excellent mechanical flexibility can further open up new multifunctional applications, such as wearable communication, biomedical diagnosis and personal health monitoring with human-friendly interfaces.<sup>3–5</sup> As a result, self-powered flexible optoelectronic sensing systems have been demonstrated to be the core of next-generation sensor networks due to their lightweight, self-sufficient and long-term properties with bendable and conformable construction to arbitrary surface topology, which are urgently needed for deformation tolerant, sustainable, maintenance-free and long-term operations especially in unattended harsh environment.

As indispensable components of optoelectronic sensing, UV photoswitches or photodetectors have a wide range of commercial applications, such as biological and chemical

analysis, flame monitoring, missile detection, secure space communication, and astronomical studies. Nowadays, the use of low-dimensional wide-bandgap semiconductor nanomaterials, such as GaN, ZnO,  $\beta$ -Ga<sub>2</sub>O<sub>3</sub>, TiO<sub>2</sub> and other metal-oxide nanostructures, has attracted intense attention to develop flexible UV photoswitches or detectors with highly enhanced responsivity and photoconductivity gain.<sup>6–10</sup> To get the best performance, an external bias is required as the driving force to prevent the recombination of photogenerated electron–hole pairs. It is favorable to improving UV response characteristics (e.g., photoresponsivity and response speed) relative to zero-bias UV detection.<sup>7,11</sup> Moreover, because of high surface-to-volume ratio, the surface dominated photocurrent transport also plays a great role in UV detection based on these nanostructured semiconductors. It is highly sensitive to the ambient environment such as atmosphere, temperature, humidity and so on, thus inducing the signal fluctuation and poor selectivity disadvantageous for long-term and stable UV

Received: November 16, 2015

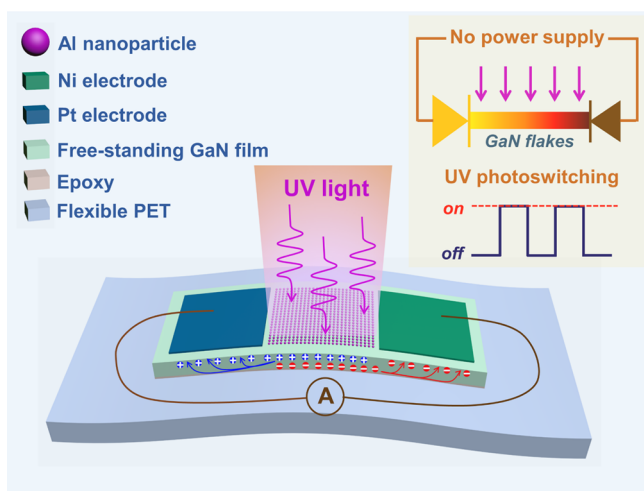
Accepted: December 15, 2015

detection.<sup>12,13</sup> To resolve these bottlenecks, GaN thin film-based UV sensors have great advantages of being bulk-dominated optical response, all-solid-state, good chemical and thermal stability, robust radiation hardness, and long lifetime.<sup>14–17</sup> To realize high-performance self-powered UV detection, the optimal design of GaN-based heterojunctions can be utilized to produce a built-in electric field or a piezoelectric field instead of external bias, which effectively makes the photogenerated electron–hole pairs separate and drift to the external circuit. However, high-performance GaN-based devices are often rigid on nonflexible substrates (such as sapphire, silicon carbide, silicon) due to the high fabrication temperature. Such limitation seriously obstructs the fast growing demand of related flexible or wearable applications.

In this work, we developed a flexible self-powered GaN membrane-based metal–semiconductor–metal (MSM) UV photoswitch by substrate transferring technique. The asymmetric MSM structure was well designed to effectively suppress carrier recombination and enhance carrier transport, which had a direct influence to the device performance of self-powered UV photoresponse. In combination with UV absorption enhancement of Al nanoparticle array, we have achieved a highly sensitive UV response and high on/off ratio. At self-powered condition (no external bias), its UV on/off ratio reaches up to  $4.67 \times 10^5$  with high reliability of on/off switching response. Also its UV detection shows an excellent sensitivity ( $1.78 \times 10^{12} \text{ cm}\cdot\text{Hz}^{0.5}\text{W}^{-1}$ ). On the basis of piezoelectric polarization engineering, strain modulation can further improve the UV on/off ratio ( $\sim 154\%$ ) by piezophototronic effect. The piezo-phototronic effect is to use piezopotential to tune/modulate the generation, separation, diffusion and recombination of electron–hole pairs during optoelectronic processes.<sup>12,18–22</sup> Such tunability offers an effective way to enhance the on/off response performances of the flexible UV photoswitch device, which will promote the development of self-powered flexible optoelectronic devices and integrated systems.<sup>5,23,24</sup>

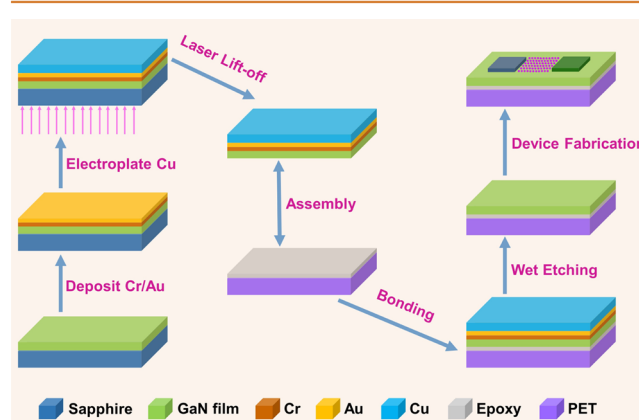
## RESULTS AND DISCUSSION

Figure 1 shows a schematic diagram of a self-powered GaN flexible film-based MSM UV photoswitch device. The GaN flexible film on PET substrate was obtained by substrate



**Figure 1.** Schematic diagram of a self-powered GaN flexible film-based MSM UV photoswitch device.

transferring technique, which will be discussed later in Figure 2. The flexible GaN-based photoswitch was designed and



**Figure 2.** Fabrication flowchart of GaN flexible film-based MSM photoswitch.

fabricated by unsymmetrical MSM structure. The Pt and Ni electrodes were deposited on each sides of GaN flexible film. Between them, we adopted an ordered Al nanoparticle array on *c*-face GaN active layer to enhance the UV absorption.<sup>16,25</sup> Its diameter and period are about 50 and 100 nm as shown in the SEM image of Figure S1, respectively. When illuminating by UV light, the photogenerated carriers will be collected at nearby Schottky electrodes due to both the built-in and external electric fields. In particular, the photoexcited electrons and holes can move toward the opposite directions at the self-powered mode, thus forming an electrical current in external circuit. It can be expected that the interface engineering may play a great role on the performance improvement of self-powered UV photosensing by optimizing the energy band profile, barrier height, space charge region, and strain-induced piezopotential. In combination with an extremely low dark current, the self-powered photoswitch device can achieve an extremely high UV on/off ratio. Such sensor is suitable for long-term, real-time response and power free UV monitoring.

The GaN flexible membrane-based MSM photoswitch was fabricated as the flowchart in Figure 2. First, a [0001]-oriented GaN film was grown on a *c*-plane bipolar sapphire substrate by a low-pressure metal organic chemical vapor deposition system. Second, Cr/Au metal was deposited on the surface of GaN film, which served as the seeding layer for Cu electroplating. The Cr/Au/Cu metal layers offer good mechanical ductility during the transferring GaN film processing. Third, laser lift-off technique was utilized to detach the GaN/Cr/Au/Cu film from hard sapphire substrate.<sup>26–28</sup> Fourth, we transferred the GaN/Cr/Au/Cu film onto the PET substrate by bonding together with hard epoxy resins. Fifth, the Cr/Au/Cu metals on the GaN surface were removed sequentially by wet etching processes according to the Experimental Section. Finally, the MSM-based photoswitch was fabricated by depositing asymmetric Schottky Pt and Ni electrodes and Al nanoparticle array.

Furthermore, we have investigated the UV photoresponse characteristic of as-fabricated flexible GaN MSM photoswitch device. As shown in Figure 3a, it is obvious that IV characteristic in darkness shows a typical MSM transport property. There exist two Schottky barriers, one is formed at Pt/GaN interface and the other is formed at Ni/GaN

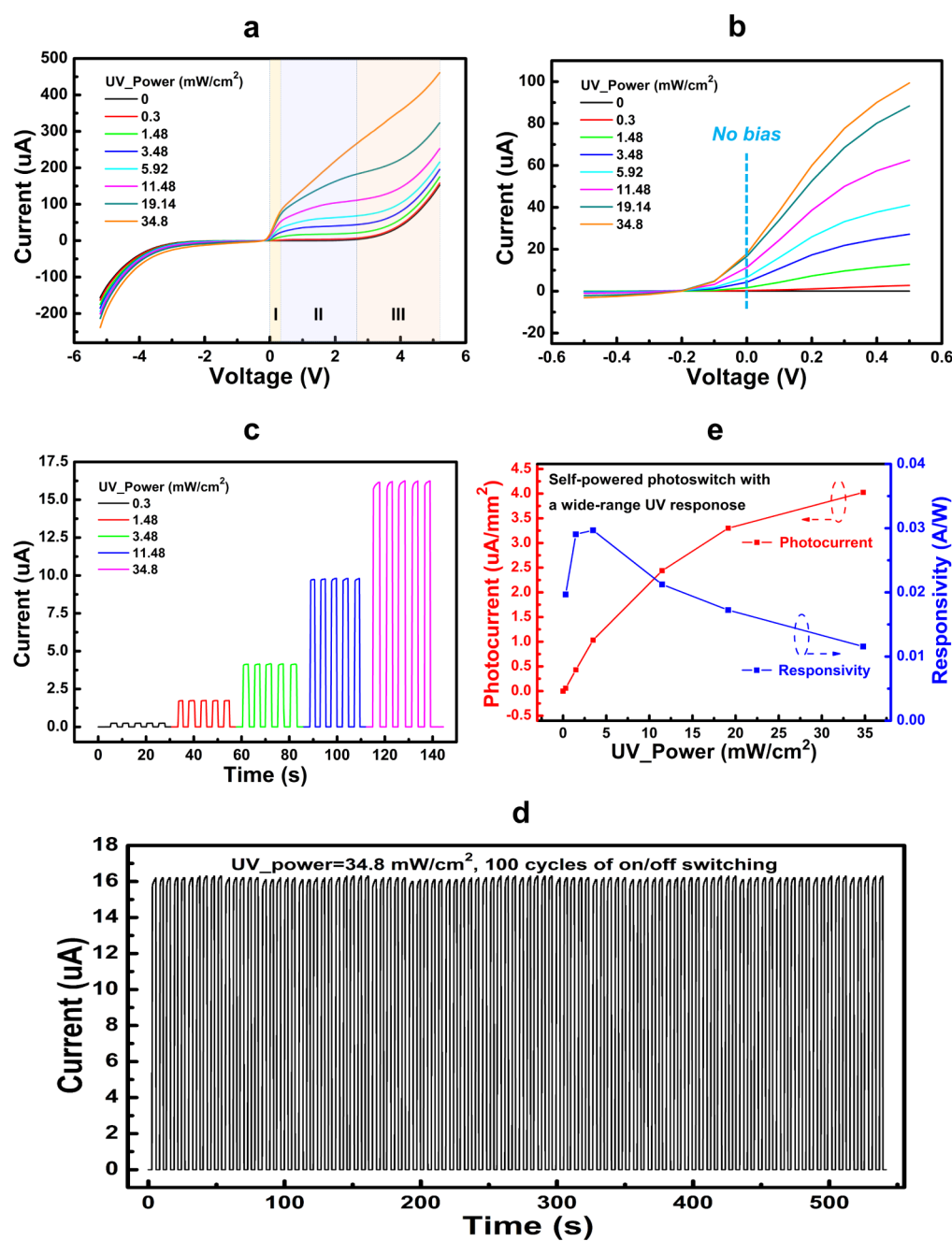


**Figure 3.** (a) The current–voltage curves of GaN flexible film-based MSM photoswitch under different UV light powers at room temperature. (b) Its current–voltage curves under different UV light powers at low bias voltage, especially 0 V for self-powered condition. (c) Its self-powered on/off switching response as a function of the UV light power at 0 V bias. (d) The repeatability of the self-powered photoswitching response at 0 V bias under 100 cycles of on/off switching under high UV illumination of 34.8 mW/cm<sup>2</sup>. (e) Its self-powered photocurrent and responsivity as a function of UV light power at 0 V bias.

interfaces. Due to the back-to-back MSM structure, leakage current has an extremely low value, which guarantees high performance for optical sensing.<sup>29–31</sup> Under UV light illumination, the photocurrent response increases gradually as the increase of UV optical power. Moreover, it exhibits an asymmetric trend at positive and negative bias voltage, respectively. The asymmetric trend of  $I$ – $V$  curves has a great dependence on the electrode metals of MSM structure, as compared in Figure 3a and Figure S2. It is noted that a stronger UV photoresponse is observed at positive bias. Additionally, there exist three UV photoresponse regions including low-voltage (I), medium-voltage (II) and high-voltage (III), as

labeled in Figure 3a. With the increasing of positive bias voltage, UV photocurrent increased dramatically in low-voltage region and gradually saturates in medium-voltage region. It demonstrates that the photogenerated electron–hole pairs can be effectively separated by the formed built-in electric field of MSM structure while keeping an extremely low dark current. Such excellent photoresponse characteristic in low-voltage region is suitable for UV photoswitching applications with high on/off ratio. However, in high-voltage region, the reverse leakage of Pt/GaN Schottky junction plays a dominant role for current transport. Both dark current and photocurrent show a

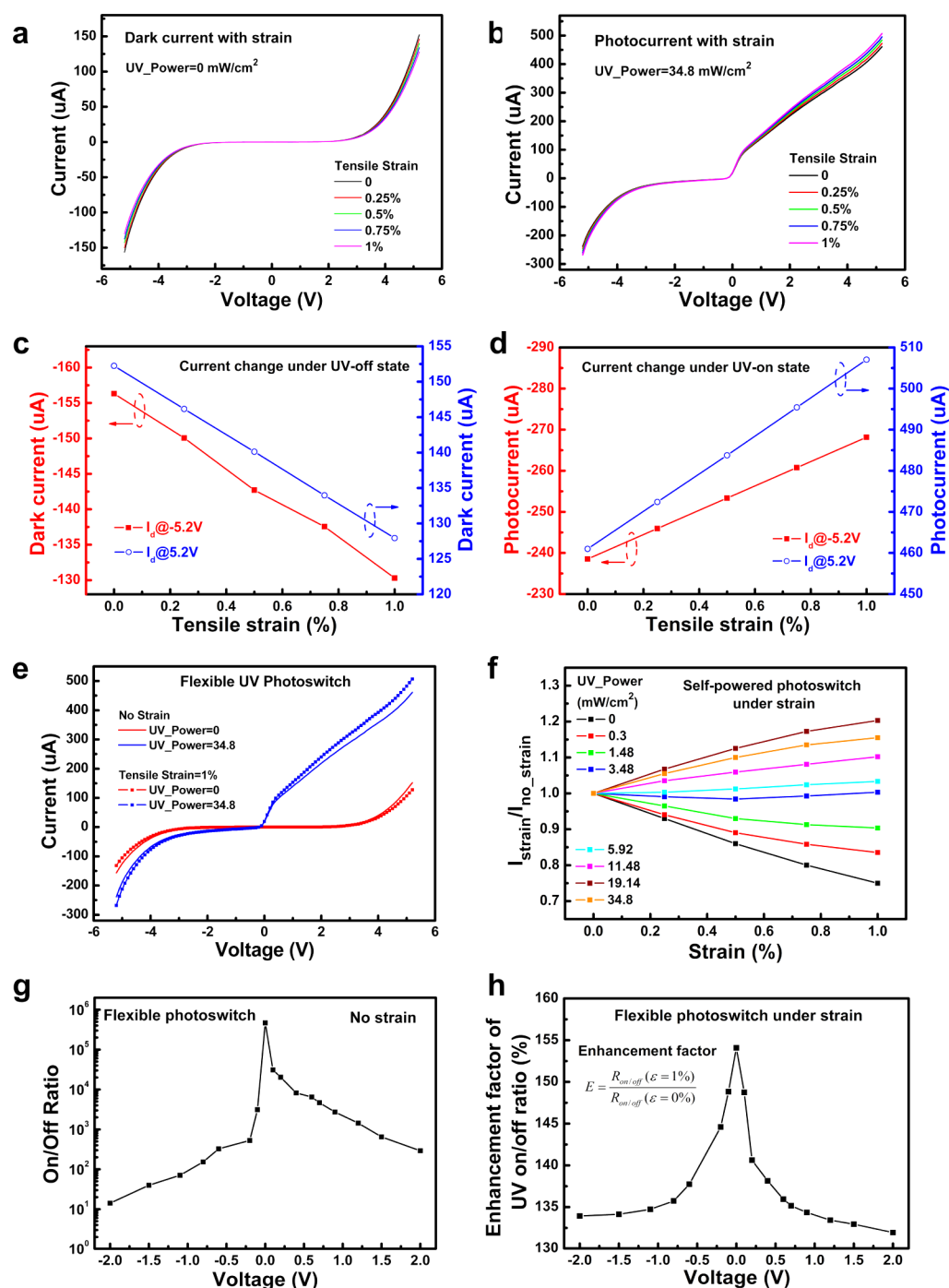


**Figure 4.** Change of current–voltage characteristics of flexible MSM photoswitch under dark (a) and UV power of 34.8 mW/cm<sup>2</sup> (b) at different tensile strains. The change of dark current (c) and photocurrent (d) at -5.2 and 5.2 V bias voltage as a function of tensile strain. (e) Its current–voltage characteristics at UV-on and UV-off states influenced by the strain-modulation effect. (f) The ratio of device currents with strain and no strain as a function of strain for different UV light powers at self-powered condition. (g) Dependence of the UV on/off ratio of our flexible MSM photoswitch on bias voltage. (h) The piezo-phototronic enhancement of the UV on/off ratio under different bias voltages. The applied strain is 1%.

fast increasing, thus deteriorating the UV photoresponse performances.

The asymmetric trend of  $I$ - $V$  curves has a great dependence on the electrode metals of MSM structure. When we adopt Pt (5.65 eV) and Ni (4.95 eV) Schottky metals with different work function, the spatial distribution of electric field is unsymmetrical in photoabsorption region at 0 V bias voltage. Both the built-in electric field and the width of depletion region are

larger at the Pt/GaN junction than those at the Ni/GaN junction. Therefore, in comparison with Ni/GaN junction, Pt/GaN junction will absorb more portion of UV light and then effectively separate the electron–hole pairs to generate photocurrent. The design of asymmetric MSM structure is crucial to obtain high-performance self-powered UV optical detection. Figure 3b presents the enlarged  $I$ - $V$  curves near 0 V. It can be seen that the asymmetric MSM photoswitch has an

obvious photocurrent response to UV light even without bias or power supply. The photocurrent response is closely related to the amplitude of the built-in electric field and the amount of photoinduced carriers. At bias voltage of 0 V in Figure 3b, its photocurrent increases from  $3.53 \times 10^{-11}$  A at dark to  $1.66 \times 10^{-5}$  A at  $34.8 \text{ mW/cm}^2$ . Correspondingly, the open-circuit voltage induced by UV illumination can reach to  $\sim 200$  mV based on photovoltaic effect. In addition, the self-powered photoswitching performance at 0 V bias has been investigated in Figure 3c. Both UV optical power and on/off switch states are modulated to study the transient response of our UV photoswitch device. The output current presents impressive consistency and repeatability for wide range of UV illumination. In Figure 3c, it exhibits a fast and wide-range response to UV illumination from several  $\mu\text{W/cm}^2$  to  $\sim 35 \text{ mW/cm}^2$ . Taking the time resolution of the testing system into consideration, the actual response time and decay time of self-powered UV photoswitch would be less than 0.1 s.<sup>28</sup> So our UV photoswitch can work well at self-powered mode with an excellent on/off photoswitching characteristic. Unlike single nanowire or nanowire array photodetectors,<sup>8,9,13,18</sup> its photoswitching response at 0 V bias keeps stable and has ultralow photocurrent fluctuation with standard deviation of  $6.64 \times 10^{-8}$  A under hundreds of on/off cycles in Figure 3d, high repeatability of which is suitable for long-term, reliable and highly sensitive UV detection/monitoring. Meanwhile, the UV detection based on large-size membrane can achieve high current output for facile and accurate measurement, avoiding the weak optical absorption and charge disturbances often happened in optical detection of nanowires or two-dimensional nanosheets.<sup>32,33</sup> According to Figure 3e, the UV photocurrent density at 0 V bias has a linear relationship with the optical power at low UV power, and increases slow-down as the UV power increases. The photoelectric responsivity ( $R$ ) of our self-powered photoswitch reaches to 0.03 A/W at low UV power ( $< 3.5 \text{ mW/cm}^2$ ), and gradually reduces to 0.0116 A/W at high UV power ( $\sim 35 \text{ mW/cm}^2$ ). The normalized detectivity ( $D^*$ ) is defined as<sup>34</sup>

$$D^* = R / \sqrt{2 e J_d} \quad (1)$$

where  $R$  and  $J_d$  are the responsivity and the dark current density of the UV photoswitch device, respectively. So a very high detectivity of  $1.78 \times 10^{12} \text{ cm} \cdot \text{Hz}^{0.5} \text{ W}^{-1}$  can be achieved at self-powered mode, which reflects excellent UV sensitivity of self-powered asymmetric MSM photoswitch.

As a suitable surface-mounted device, the flexible MSM photoswitch can be conformable to the bent objects with a certain curvature as shown in Figure S3. The strain-modulation effect on the UV on/off response performances has been well investigated. Figure 4 presents the change of the dark current (a) and UV photocurrent (b) at different tensile strains. Under UV-off state, the dark currents at positive and negative bias voltage are gradually reduced as the tensile strain increases from 0% to 1%. As shown in Figure 4c, it decreases from 152.24 to 127.94  $\mu\text{A}$  at 5.2 V and from  $-156.31$  to  $-130.29 \mu\text{A}$  at  $-5.2$  V. Both of them have similar variation amplitudes of dark current. On the other hand, when the flexible MSM photoswitch is at UV-on state with optical power of  $34.8 \text{ mW/cm}^2$ , the UV photocurrent can be enhanced a little as the increase of tensile strain. At positive bias voltage of 5.2 V, it increases from 460.98  $\mu\text{A}$  at no strain to 507.04  $\mu\text{A}$  at tensile strain of 1%, correspondingly increasing from  $-238.54$  to

$-268.14 \mu\text{A}$  at negative bias voltage of  $-5.2$  V in Figure 4d. So the photocurrent at positive bias voltage increases larger than that at negative one. More interestingly, it is noted that the strain-modulation effect at UV-on and UV-off states exists an opposite trend as compared in Figure 4e. As for the self-powered mode without bias voltage, it is found that the current change depends on both the applied strain and optical power of UV illumination in Figure 4f. At low UV illumination, the increase of Schottky barrier height (SBH) induced by tensile strain reduces the leakage current of reversed-biased Pt/GaN and Ni/GaN Schottky contacts, which dominates in the current reduction of  $I$ - $V$  characteristic. As increasing the optical power of UV illumination, photogenerated electron-hole pairs are much easier and efficient to separate apart by increasing built-in electric field under the external tensile strain, thus improving the photocurrent output. The photocurrent enhancement reaches to the maximum value of  $\sim 120\%$  under UV power of  $19.1 \text{ mW/cm}^2$  with 1% strain. It begins to weaken at higher UV power of  $34.8 \text{ mW/cm}^2$ , which is due to the partial screening of the strain-induced polarization charges by the UV photoinduced carriers.<sup>35</sup> Accordingly, it further reveals that the piezophototronic effect, rather than piezoresistive effect, plays an important role on the photoelectric response of UV photoswitch. Utilizing the strain-induced piezoelectric polarization charges presented at the vicinity of M-S contact, piezophototronic effect can tune/control the charge carriers transport process by modulating the SBHs at the local Schottky interfaces.<sup>19,36</sup> It has been used to modulate/control carrier generation, transport, separation, and recombination in light-emitting diodes or solar cells.<sup>20,21</sup> In our results, it further demonstrates that the piezo-phototronic effect provides an effective approach to improve the on/off switching performance of MSM-structured photoswitch.

Moreover, the UV on/off ratio is a crucial parameter of the photoswitch device, which can evaluate its photoswitching performance. Electrical current of our flexible MSM photoswitch is highly sensitive to UV radiation, which has a large change when exposed to and shielded from the UV radiation. As shown in Figure 4g, the UV on/off ratio of our flexible MSM photoswitch reaches to the highest value of  $4.67 \times 10^5$  at self-powered condition, which is much larger than that of GaN nanowire-based UV photodetectors using photoconductive, p-i-n, or core-shell structures.<sup>9,37</sup> So it demonstrates an excellent photosensitive characteristic without external power supply. Meanwhile, this kind of self-powered UV detection is very safe from the hazard of UV irradiation, and self-sufficient with low cost and easy maintenance for a long-time use. In addition, the UV on/off ratio has a great dependence on the bias voltage in Figure 4g. It reduces as the positive or negative bias voltage increases. Around 0 V, the high UV on/off ratio of  $3.1 \times 10^4$  and  $2.03 \times 10^4$  can be also obtained at low bias voltage of 0.1 and 0.2 V, respectively. And the UV on/off ratio still keeps above 3 orders of magnitude until the positive bias voltage of 1.2 V. However, on the side of negative bias voltage, it declines faster and drops down to 14.13 at  $-2$  V. So it demonstrates that work voltage at 0 V or low bias voltage is advantageous to highly photosensitive applications. To verify the piezo-phototronic enhancement of UV on/off ratio, the UV on/off performance has been examined by applying external strains to our flexible photoswitch device. By exerting a tensile strain of 1%, the UV on/off ratio can be partially enhanced as seen in Figure 4h. The enhancement factor of UV on/off ratio is defined as

$$E = \frac{R_{\text{on/off}}(\varepsilon = 1\%)}{R_{\text{on/off}}(\varepsilon = 0\%)} \quad (2)$$

It is the specific value of the UV on/off ratio under 1% and 0% strains. In the whole bias voltage from  $-2$  to  $2$  V, the strain-tuned enhancement takes effect with the enhancement factor of  $>130\%$ . It appears a peak value of  $154\%$  around  $0$  V, exhibiting a stronger strain-tuned UV on/off ratio at self-powered mode. Therefore, our flexible photoswitch can undertake a little strain to enhance the UV on/off switching performance.

To evaluate the strain modulation on photoresponse properties, we study the electrical transport behaviors of our flexible photoswitch device with external strain and UV irradiation. The asymmetric MSM structure of as-fabricated Pt/GaN/Ni photoswitch consists of two back-to-back Schottky barriers, which is vital to its UV optical absorption and electrical transport. Both Pt and Ni metals formed good Schottky contacts with Ga-face GaN flexible film, which act as source and drain electrodes, respectively. Figure 5a presents the band diagram of asymmetric Pt/GaN/Ni device in equilibrium state without bias voltage and external strain. Due to different SBHs of two Schottky contacts, both built-in electric field and the width of depletion region are larger at Pt/GaN junction than that at Ni/GaN junction. So the incident UV light is mostly absorbed at Pt/GaN region. More importantly, the photo-

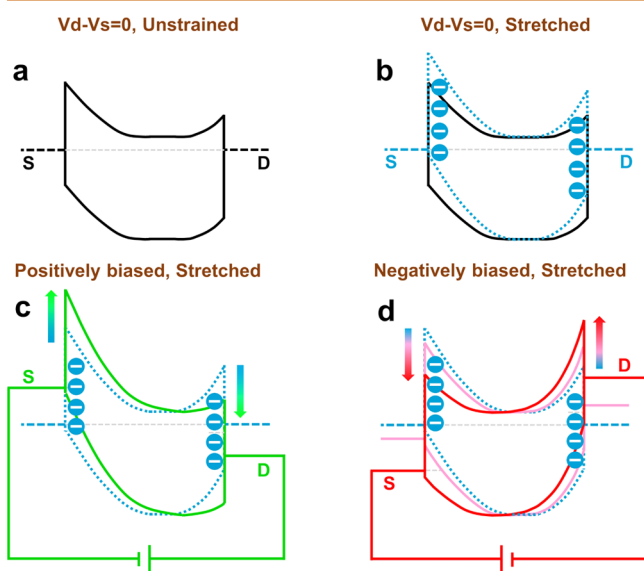


**Figure 5.** Band diagram of asymmetric Pt/GaN/Ni device. (a) In equilibrium state without bias voltage and external strain, there exist two Schottky contacts with different SBHs indicated by dark solid line. The asymmetric electric fields produce the total loop-circuit current for self-powered UV detection. (b) Without bias voltage, when applying tensile strains to flexible GaN membrane with (0001)-polarity, negative piezoelectric charges are created at two Schottky junctions indicated by blue dashed line. (c) When the photoswitch is positively biased and stretched, both SBH and depletion width of Pt/GaN Schottky junction are increased while that of Ni/GaN are decreased. Its asymmetry is enhanced as indicated by green solid line. (d) The photoswitch is negatively biased and stretched. The symmetric band structure indicated by pink solid line acts as a critical point, which is achieved by the combined action of the built-in electric field, strain-induced piezopotential and external bias voltage. The asymmetry of MSM-structure is weakened before the critical point while increased again after the critical point as shown by red solid line.

induced electrons and holes are quickly separated away due to the stronger electric field at Pt/GaN side. And they move toward the Ni and Pt electrode, respectively, thus producing the total loop-circuit current for self-powered UV detection. Furthermore, when applying tensile strain to flexible GaN membrane with (0001)-polarity, negative piezoelectric charges are generated at interfaces of Pt/GaN and Ni/GaN, as indicated by the blue dashed line in Figure 5b. The SBHs at these two junctions are increased simultaneously, which makes the free carriers difficult to transport from source to drain.<sup>12,38</sup> It is consistent with the experimental result that the dark current decreases as the increase of tensile strain in Figure 4a. When UV illuminated at Pt/GaN and Ni/GaN Schottky barriers, the photocurrent response is dependent on the optical absorption, separation, recombination of photogenerated carriers. The increased built-in electric field and depletion width are beneficial to promoting space separation and suppressing recombination of photogenerated electron–hole pairs. Correspondingly, the enhanced photocurrent response has been achieved by tensile strain-induced piezopotential of Pt/GaN and Ni/GaN Schottky barrier as shown in Figure 4b.

To further verify the proposed physical mechanism, the external electric field is taken into consideration to understand the asymmetric photoresponse characteristic based on asymmetric MSM-structure photoswitch. Here, the induced piezopotential at Pt/GaN and Ni/GaN Schottky barrier is stable by applying fixed tensile strain to the flexible GaN flake. When the photoswitch is positively biased in Figure 5c, both SBH and depletion width of Pt/GaN Schottky junction are increased, while that of Ni/GaN Schottky junction are decreased with the increasing of bias voltage. The asymmetry of MSM band structure is gradually enhanced, which leads to improving photocurrent response as shown by green solid line in Figure 5c. On the contrary, when the photoswitch is negatively biased in Figure 5d, the SBH of Ni/GaN increases, while that of Pt/GaN decreases with the increasing of biased voltage. It is obvious that the MSM band structure has an asymmetric-symmetric-asymmetric transition. In Figure 5d, the symmetric band structure is achieved by the combined action of the built-in electric field, strain-induced piezopotential and external bias voltage, which acts as a critical point indicated by pink solid line. It can be seen that when the bias voltage is increased, the asymmetry of MSM-structure is weakened before the critical point while increased again after the critical point, as shown by red solid line in Figure 5d. In comparison with negatively biased condition, there exist higher UV photoresponse and UV on/off ratio at positive bias in consistency with our experimental results. It further confirms that the asymmetric distribution of electric field in asymmetric MSM structure plays a significant role for photoelectric conversion.

## CONCLUSIONS

In summary, a flexible and self-powered MSM-based photoswitch was successfully fabricated using the flexible GaN membrane on PET. Even without external electrical field, the photogenerated electron–hole pairs can be effectively separated by the formed built-in electric field of asymmetric MSM structure. On the basis of asymmetric MSM structure, our GaN-based MSM photoswitch works well at self-powered mode with excellent photoresponse to UV illumination. Its responsivity and detectivity are  $0.03$  A/W and  $1.78 \times 10^{12}$  cm<sup>2</sup>·Hz<sup>0.5</sup>·W<sup>−1</sup>, respectively. There is no need of external power for self-powered UV sensing, which is suitable for long-term,

reliable and highly sensitive UV detection/monitoring. In addition, it has good mechanical flexibility for strain modulation. On the basis of the piezo-phototronic effect, the enhancement of UV on/off ratio up to 154% at 0 V is observed by applying small strain of 1%. Therefore, our study provides a potential approach to enhance/optimize the performances of self-powered optoelectronic devices by the piezo-phototronic effect, which could be of interest for flexible and self-powered optoelectronic sensing applications.

## EXPERIMENTAL SECTION

The [0001]-oriented GaN film was grown on a c-plane bipolished sapphire substrate by a low-pressure metal organic chemical vapor deposition system. Low-temperature nucleation and then high-temperature growth were implemented to obtain high-quality undoped GaN thin film. The whole fabrication of the GaN flexible membrane-based MSM photoswitch was presented in Figure 2. Chromium/gold (Cr/Au) seeding layers were deposited on the (0001)-face of GaN film by electron beam evaporation. And then, a copper (Cu) supporting layer with thickness of 80  $\mu\text{m}$  was electroplated on the Cr/Au seeding layers. After that, the GaN film was detached from the sapphire substrate by laser lift-off. The obtained GaN/Cr/Au/Cu film could be transferred to flexible substrates as follows: First, it was bonded tightly with the transparent polyethylene terephthalate (PET) by hard epoxy resins. Second, the Cu supporting layer was removed completely by ammonium hydroxide ( $\text{NH}_4\text{OH}$ ) and hydrogen peroxide ( $\text{H}_2\text{O}_2$ ) mixture solution. Third, the Au and Cr metal layer were etched sequentially by *aqua regia*, nitric acid and ammonium ceric nitrate mixed solutions. Finally, the UV photoswitch device was fabricated by using the GaN/PET flexible film. The dot matrix of aluminum (Al) nanoparticles were defined with diameter of 50 nm and period of 100 nm on the (0001)-face GaN surface by electron beam lithography. The active area for optical detection is 1  $\text{mm}^2$ . And then, the platinum (Pt) and nickel (Ni) metals for Schottky contacts were deposited at two sides of active region by electron beam evaporation. So this asymmetric MSM device structure has been developed for flexible UV photoswitching applications. Figure 1 presented the schematic diagram of photoelectric test setup of a self-powered GaN flexible film-based MSM UV photoswitch device. Direct current supply and electrical testing were carried out by using a Keithley 2400 source meter. A high-voltage mercury lamp was selected as a good UV optical source for photoresponse and photoswitching measurements at room temperature. Its emission range was below 400 nm regulated by optical filter. The incident optical power was calibrated by UV power meter (Thorlabs PM100D). A displacement stage was used to introduce the external strain in GaN film for the study of strain modulation effect.

## ASSOCIATED CONTENT

### Supporting Information

The Supporting Information is available free of charge on the ACS Publications website at DOI: 10.1021/acsnano.5b07217.

More detailed information about the ordered Al nanoparticle array for the enhancement of UV absorption; the UV photoresponse of symmetric MSM device fabricated by Pt-GaN flexible membrane-Pt structure, and the flexibility of self-powered GaN-based UV photoswitch (PDF)

## AUTHOR INFORMATION

### Corresponding Authors

\*E-mail: jyzhai@binn.cas.cn.

\*E-mail: zlwang@gatech.edu.

### Notes

The authors declare no competing financial interest.

## ACKNOWLEDGMENTS

This work was supported by NSFC 51472056, 51402064, the “thousands talents” program for pioneer researcher and his innovation team, China, the Recruitment Program of Global Youth Experts, China and Youth Innovation Promotion Association of Chinese Academy of Sciences (2015387).

## REFERENCES

- (1) Wang, Z. L. Toward Self-Powered Sensor Networks. *Nano Today* **2010**, *5*, 512–514.
- (2) Wang, Z. L. Self-Powered Nanosensors and Nanosystems. *Adv. Mater.* **2012**, *24*, 280–285.
- (3) Ruh, D.; Reith, P.; Sherman, S.; Theodor, M.; Ruhhammer, J.; Seifert, A.; Zappe, H. Stretchable Optoelectronic Circuits Embedded in a Polymer Network. *Adv. Mater.* **2014**, *26*, 1706–1710.
- (4) Russev, M. M.; Hecht, S. Photoswitches: From Molecules to Materials. *Adv. Mater.* **2010**, *22*, 3348–3360.
- (5) Rogers, J. A.; Someya, T.; Huang, Y. G. Materials and Mechanics for Stretchable Electronics. *Science* **2010**, *327*, 1603–1607.
- (6) Li, Y. B.; Tokizono, T.; Liao, M. Y.; Zhong, M.; Koide, Y.; Yamada, I.; Delaunay, J. J. Efficient Assembly of Bridged  $\beta\text{-Ga}_2\text{O}_3$  Nanowires for Solar-Blind Photodetection. *Adv. Funct. Mater.* **2010**, *20*, 3972–3978.
- (7) Xie, Y. R.; Wei, L.; Li, Q. H.; Chen, Y. X.; Liu, H.; Yan, S. S.; Jiao, J.; Liu, G. L.; Mei, L. M. A High Performance Quasi-Solid-State Self-Powered UV Photodetector Based on  $\text{TiO}_2$  Nanorod Arrays. *Nanoscale* **2014**, *6*, 9116–9121.
- (8) Tian, W.; Zhang, C.; Zhai, T. Y.; Li, S. L.; Wang, X.; Liu, J. W.; Jie, X.; Liu, D. Q.; Liao, M. Y.; Koide, Y. S.; Golberg, D.; Bando, Y. Flexible Ultraviolet Photodetectors with Broad Photoresponse Based on Branched ZnS-ZnO Heterostructure Nanofilms. *Adv. Mater.* **2014**, *26*, 3088–3093.
- (9) González-Posada, F.; Songmuang, R.; Hertog, M. D.; Monroy, E. Room-Temperature Photodetection Dynamics of Single GaN Nanowires. *Nano Lett.* **2012**, *12*, 172–176.
- (10) Shi, X. Q.; Peng, M. Z.; Kou, J. Z.; Liu, C. H.; Wang, R.; Liu, Y. D.; Zhai, J. Y. A Flexible GaN Nanowire Array-Based Schottky-Type Visible Light Sensor with Strain-Enhanced Photoresponsivity. *Adv. Electron. Mater.* **2015**, DOI: 10.1002/aeml.201500169.
- (11) Hatch, S. M.; Briscoe, J.; Dunn, S. A Self-Powered ZnO-Nanorod/CuSCN UV Photodetector Exhibiting Rapid Response. *Adv. Mater.* **2013**, *25*, 867–871.
- (12) Yu, R. M.; Niu, S. M.; Pan, C. F.; Wang, Z. L. Piezotronic Effect Enhanced Performance of Schottky-Contacted Optical, Gas, Chemical and Biological Nanosensors. *Nano Energy* **2015**, *14*, 312–339.
- (13) Peng, L.; Hu, L. F.; Fang, X. S. Low-Dimensional Nanostructure Ultraviolet Photodetectors. *Adv. Mater.* **2013**, *25*, 5321–5328.
- (14) Nakamura, S. In *The Blue Laser Diode: The Complete Story*; Nakamura, S., Pearsall, S. J., Fasol, G., Eds.; Springer: Berlin, Germany, 2000, Ch. 1.
- (15) Pimputkar, S.; Speck, J. S.; DenBaars, S. P.; Nakamura, S. Prospects for LED Lighting. *Nat. Photonics* **2009**, *3*, 180.
- (16) Li, D. B.; Sun, X. J.; Song, H.; Li, Z. M.; Chen, Y. R.; Jiang, H.; Miao, G. Q. Realization of a High-Performance GaN UV Detector by Nanoplasmonic Enhancement. *Adv. Mater.* **2012**, *24*, 845–849.
- (17) Cheng, G.; Wu, X. H.; Liu, B.; Li, B.; Zhang, X. T.; Du, Z. L. ZnO Nanowire Schottky Barrier Ultraviolet Photodetector with High Sensitivity and Fast Recovery Speed. *Appl. Phys. Lett.* **2011**, *99*, 203105.
- (18) Yang, Q.; Guo, X.; Wang, W.; Zhang, Y.; Xu, S.; Lien, D. H.; Wang, Z. L. Enhancing Sensitivity of a Single ZnO Micro/Nanowire Photodetector by Piezo-Phototronic Effect. *ACS Nano* **2010**, *4*, 6285–6291.
- (19) Wang, Z. L. Progress in Piezotronics and Piezo-Phototronics. *Adv. Mater.* **2012**, *24*, 4632–4646.
- (20) Peng, M. Z.; Li, Z.; Liu, C. H.; Zheng, Q.; Shi, X. Q.; Song, M.; Zhang, Y.; Du, S. Y.; Zhai, J. Y.; Wang, Z. L. High-Resolution Dynamic

Pressure Sensor Array Based on Piezo-Phototronic Effect Tuned Photoluminescence Imaging. *ACS Nano* **2015**, *9*, 3143–3150.

(21) Yang, Q.; Wang, W. H.; Xu, S.; Wang, Z. L. Enhancing Light Emission of ZnO Microwire-Based Diodes by Piezo-Phototronic Effect. *Nano Lett.* **2011**, *11*, 4012–4017.

(22) Peng, M. Z.; Zhang, Y.; Liu, Y. D.; Song, M.; Zhai, J. Y.; Wang, Z. L. Magnetic-Mechanical-Electrical-Optical Coupling Effects in GaN-Based LED/Rare-Earth Terfenol-D Structures. *Adv. Mater.* **2014**, *26*, 6767–6772.

(23) Hwang, G.-T.; Im, D.; Lee, S. E.; Lee, J.; Koo, M.; Park, S. Y.; Kim, S.; Yang, K.; Kim, S. J.; Lee, K.; Lee, K. J. *In Vivo* Silicon-Based Flexible Radio Frequency Integrated Circuits Monolithically Encapsulated with Biocompatible Liquid Crystal Polymers. *ACS Nano* **2013**, *7*, 4545–4553.

(24) Park, W. I.; You, B. K.; Mun, B. H.; Seo, H. K.; Lee, J. Y.; Hosaka, S.; Yin, Y.; Ross, C. A.; Lee, K. J.; Jung, Y. S. Self-Assembled Incorporation of Modulated Block Copolymer Nanostructures in Phase-Change Memory for Switching Power Reduction. *ACS Nano* **2013**, *7*, 2651–2658.

(25) Atwater, H. A.; Polman, A. Plasmonics for Improved Photovoltaic Devices. *Nat. Mater.* **2010**, *9*, 205–213.

(26) Lee, S. H.; Jeong, C. K.; Hwang, G. - T.; Lee, K. J. Self-Powered Flexible Inorganic Electronic System. *Nano Energy* **2015**, *14*, 111–125.

(27) Iida, D.; Kawai, S.; Ema, N.; Tsuchiya, T.; Iwaya, M.; Takeuchi, T.; Kamiyama, S.; Akasaki, I. Laser Lift-Off Technique for Free-standing GaN Substrate Using an In Droplet Formed by Thermal Decomposition of GaInN and Its Application to Light-Emitting Diodes. *Appl. Phys. Lett.* **2014**, *105*, 072101.

(28) Cho, H. K.; Kim, S. K.; Bae, D. K.; Kang, B. C.; Lee, J. S.; Lee, Y. H. Laser Liftoff GaN Thin-Film Photonic Crystal GaN-Based Light-Emitting Diodes. *IEEE Photonics Technol. Lett.* **2008**, *20*, 2096–2098.

(29) Xie, F.; Lu, H.; Chen, D. J.; Zhang, R.; Zheng, Y. D. GaN MSM Photodetectors Fabricated on Bulk GaN with Low Dark-Current and High UV/Visible Rejection Ratio. *Phys. Status Solidi C* **2011**, *8*, 2473–2475.

(30) Yu, C. L.; Chang, P. C.; Chang, S. J.; Wu, S. L. High-Detectivity GaN MSM Photodetectors with Low-Temperature GaN Cap Layers and Ir/Pt Contact Electrodes. *Electrochem. Solid-State Lett.* **2007**, *10*, H171–H174.

(31) Caliskan, D.; Butun, B.; Cakir, M. C.; Ozcan, S.; Ozbay, E. Low Dark Current and High Speed ZnO Metal-Semiconductor-Metal Photodetector on SiO<sub>2</sub>/Si Substrate. *Appl. Phys. Lett.* **2014**, *105*, 161108.

(32) Gan, X. T.; Shiue, R. - J.; Gao, Y.; Meric, I.; Heinz, T. F.; Shepard, K.; Hone, J.; Assefa, S.; Englund, D. Chip-Integrated Ultrafast Graphene Photodetector with High Responsivity. *Nat. Photonics* **2013**, *7*, 883–887.

(33) Zhang, D. Y.; Gan, L.; Cao, Y.; Wang, Q.; Qi, L. M.; Guo, X. F. Understanding Charge Transfer at PbS-Decorated Graphene Surfaces Toward a Tunable Photosensor. *Adv. Mater.* **2012**, *24*, 2715–2720.

(34) Lin, C.-H.; Yu, C.-Y.; Peng, C.-Y.; Ho, W. S.; Liu, C. W. Broadband SiGe/Si Quantum Dot Infrared Photodetectors. *J. Appl. Phys.* **2007**, *101*, 033117.

(35) Wang, C. H.; Liao, W. S.; Lin, Z. H.; Ku, N. J.; Li, Y. C.; Chen, Y. C.; Wang, Z. L.; Liu, C. P. Optimization of the Output Efficiency of GaN Nanowire Piezoelectric Nanogenerators by Tuning the Free Carrier Concentration. *Adv. Energy Mater.* **2014**, *4*, 1400392.

(36) Wang, Z. L. Piezopotential Gated Nanowire Devices: Piezotronics and Piezo-Phototronics. *Nano Today* **2010**, *5*, 540–552.

(37) Consonni, V.; Feuillet, G. *Wide Band Gap Semiconductor Nanowires 2*; ISTE: London, 2014; Chapter 8.

(38) Hu, Y. F.; Zhou, J.; Yeh, P. H.; Li, Z.; Wei, T. Y.; Wang, Z. L. Supersensitive, Fast-Response Nanowire Sensors by Using Schottky Contacts. *Adv. Mater.* **2010**, *22*, 3327–3332.